

Na, K, Rb, and Cs exchange in heulandite single crystals: Diffusion kinetics

PING YANG,¹ JANO STOLZ,¹ THOMAS ARMBRUSTER,¹ AND MICKEY E. GUNTER²

¹Laboratorium für chemische und mineralogische Kristallographie, Universität Bern, Freiestrasse 3, CH-3012 Bern, Switzerland

²Department of Geology and Geological Engineering, University of Idaho, Moscow, Idaho 83844, U.S.A.

ABSTRACT

Diffusion-exchange kinetics were determined at temperatures between 320 and 425 K for Na⁺ in single crystals of natural heulandite, Na_{0.96}Ca_{3.54}K_{0.09}(Al_{8.62}Si_{27.51}O₇₂)·nH₂O, and K⁺, Rb⁺, and Cs⁺ for Na⁺ in Na-exchanged heulandite. Cation diffusion was measured on (010) cleavage plates with the aid of a polarizing microscope. This is possible because the optical properties, in particular the extinction angle, vary with the chemical composition of the channel occupants. This optical method is restricted to platy zeolites of monoclinic or triclinic symmetry where the channels are parallel to the crystal plate. Unlike conventional measurements, this method does not require the determination of the surface area of the zeolite.

No indication of anisotropic diffusion was observed on (010) plates for any of the exchanged cation pairs. Diffusion coefficients (*D*) show that the diffusion rate of Na⁺ → Ca²⁺ is much slower than those of K⁺ → Na⁺, Rb⁺ → Na⁺, and Cs⁺ → Na⁺, because of the strong Coulombic interaction of Ca²⁺ with the tetrahedral framework compared with an exchange of monovalent species. The activation energy (*E_a*) and the pre-exponential factor (*D₀*) were calculated from the variation of *D* with temperature for each diffusing cation. Comparable values of *E_a* for K⁺ → Na⁺ and Rb⁺ → Na⁺ suggest a similar diffusion process, while the lower value of *E_a*, combined with relatively low diffusion rates for Cs⁺ → Na⁺ implies a different diffusion mechanism for Cs⁺.

INTRODUCTION

The cation-exchange properties of zeolite minerals were first observed almost 100 years ago (Breck 1974). Since then, there have been many investigations of cation-diffusion mechanisms in natural and synthetic zeolites. Barrer and Hinds (1953), Barrer et al. (1963, 1967), Barrer and Munday (1971a, 1971b), Ames (1960, 1962), and Sherry (1966) have studied the cation-exchange properties of many natural zeolites (e.g., analcime, leucite, chabazite, and clinoptilolite) and many synthetic zeolites (e.g., X, Na-P, K-F). However, in most of these studies the determination of kinetic parameters mainly depended on monitoring the variation of solution concentrations accompanied by a determination of the zeolite surface area. The latter measurement is the crucial step in this technique, and surface area measurements may result to errors in *D* by three orders of magnitude (Rees and Rao 1966). The krypton adsorption method, which is frequently used to measure the surface area of a zeolite powder, may lead to incorrect results if during the measurement zeolites release H₂O or if krypton enters the structural pores (Barrer et al. 1963). In addition, experiments using powdered samples do not provide any direct information on the anisotropy of exchange kinetics. A simple effective method for the direct observation of cation diffusion in zeolite single crystals has not been reported to date.

Minerals of the heulandite structure type, heulandite

(Na,K)Ca₄(Al₉Si₂₇O₇₂)·24 H₂O and clinoptilolite (Na,K)₆(Al₆Si₃₀O₇₂)·20 H₂O, have been used for the removal of radioactive Cs⁺ and Sr²⁺ from low-level waste streams of nuclear power stations and for the extraction of ammonium in sewage because of their excellent selectivity of cation-exchange and absorption (Mumpton 1988; Smyth et al. 1990).

Heulandite belongs to the family of platy zeolites. Its framework is composed of dense (010) layers formed by four- and five-membered rings of (Si,Al) tetrahedra. These layers are connected by relatively sparse (Si,Al)-O-(Si,Al) columns. The crystal structure is characterized by three kinds of channels (Fig. 1) defined by tetrahedral rings (unit-cell setting: *a* = 17.7, *b* = 17.9, *c* = 7.4 Å, β = 116°). Channels A and B extend parallel to the *c* axis and are defined by ten- and eight-membered rings of tetrahedra, respectively (Fig. 1). Channel C, formed by another eight-membered ring, runs parallel to the *a* axis (Koyama and Takéuchi 1977) and parallel to the [102] direction (Merkle and Slaughter 1968). All channels lie parallel to (010) (Fig. 1). The channels, in turn, produce the perfect (010) cleavage found in this family of zeolites. Thus at low temperature (< 500 K), significant cation diffusion in heulandite occurs only parallel to the (010) plane. Diffusion perpendicular to (010) would force cations to penetrate five-membered rings of tetrahedra, which seems unlikely for Na⁺, K⁺, Rb⁺, and Cs⁺.

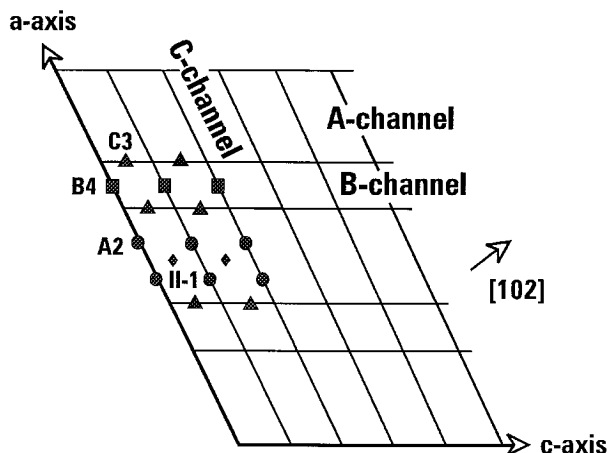


FIGURE 1. A schematic representation of the cation sites and alignment of channels in heulandite viewed down the b axis. The A and B channels are shown parallel to c and contain the A2 and B4 cation sites (normally called M1 and M2) and the new cations site II-1. The C channel is parallel to a and contains the C3 cation (normally called M3).

In a recent paper Yang and Armbruster (1996) determined the crystal structures of Na-, K-, Rb-, and Cs-exchanged varieties of heulandite studied by single-crystal X-ray diffraction data at 100 K. Three general cation positions, II-1, C3, and B4 (Fig. 1), were found in all alkali-cation-exchanged heulandite samples. For Rb- and Cs-exchanged crystals, the additional cation site A2 also occurs (Fig. 1). The letter of the cation position represents the channel (defined above) where the cations were located, and the Roman numeral represents a cage. II-1 indicates a site close to the wall of cage II, which is formed by two ten-membered A-rings and two eight-membered C-rings (Yang and Armbruster 1996). For all exchanged samples, the highest cation concentration was located at C3, near the center of an eight-membered ring formed by $(\text{Si,Al})\text{O}_4$ tetrahedra. This cation site nomenclature was developed by Yang and Armbruster (1996) to correlate a cation's location to a channel (i.e., A, B, or C) or a cage type. Past cation site designation (Gunter et al. 1994) would relate Na1 (= M1) to A2, Ca2 (= M2) to B4, K3 (= M3) to C3, while the II-1 site would be in a similar location to that of Pb5 (Gunter et al. 1994).

Tiselius (1934) showed that the rate of hydration and dehydration of heulandite single crystals under conditions of controlled vapor-pressure and temperature can be quantitatively measured by the change of optical birefringence and extinction angle on (010) crystal plates. Gunter et al. (1994) reported that the birefringence, δ (010), is 0.0010 for a natural Ca-rich heulandite, 0.0026 for a Na-exchanged heulandite, and 0.0145 for a Pb-exchanged heulandite. With $b = Z$, the extinction angle ($X : c$) changes from 7° (non-exchanged) to 19° (Na-exchanged) to 11° (Pb-exchanged). Thus the birefringence and optical orientation of the samples before and after exchange varied dramatically. These experiments indicate that cation-

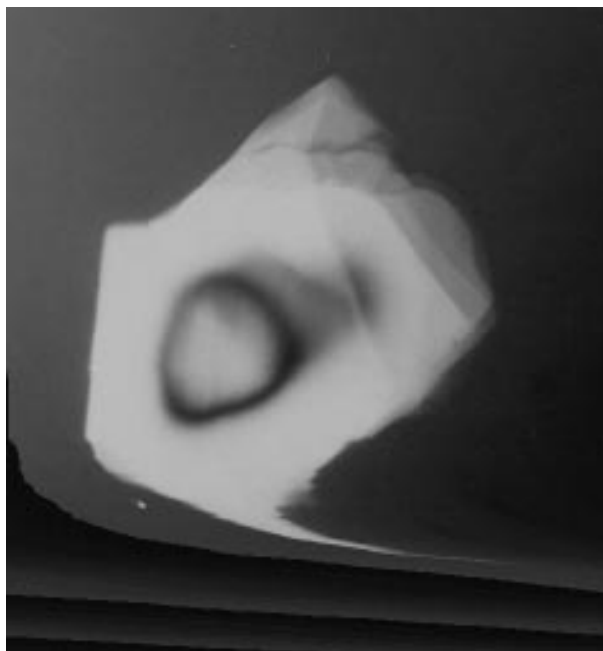


FIGURE 2. Photomicrograph taken with crossed polarizers showing Rb^+ exchange into a Na-exchanged heulandite at 330 K after 24 h. The diameter of the crystal is approximately 350 μm . The light rim of the crystal shows the Rb-exchanged zone, approximately 96 μm , and the dark boundary indicating that the exchange process had not yet been completed. Note also that the center of the crystal is not at perfect extinction but is a few degrees off. This slightly off-extinction position induces no error in the measurement of t but allows for better visual distinction of the dark boundary.

diffusion kinetics in heulandite can also be monitored with a polarizing microscope, provided that the exchanged cations lead to a variation of birefringence or extinction angle on (010).

Relative differences in the extinction angles were used herein to perform a systematic quantitative study of alkali group ions exchanged into heulandite single crystals. Thus diffusion in heulandite could be directly observed with a polarizing microscope by placing the non-exchanged core at extinction and measuring the non-extinct exchanged rim to determine the depth of cation diffusion (Fig. 2).

EXPERIMENTAL METHODS

As starting material, coarse-grained heulandite from Nasik, India (Sukheswala et al. 1974) with the composition $\text{Na}_{0.96}\text{Ca}_{3.54}\text{K}_{0.09}(\text{Al}_{8.62}\text{Si}_{27.51}\text{O}_{72}) \cdot n\text{H}_2\text{O}$ was used. The large single crystals were ground and sieved to an approximate grain size of 0.1–0.5 mm. The exchange-diffusion experiment of Na^+ with natural Ca-rich heulandite was carried out by heating heulandite samples in 2M NaCl solution. A teflon-coated autoclave was used for high temperature exchange experiments (> 373 K). The other exchange-diffusion experiments were performed by

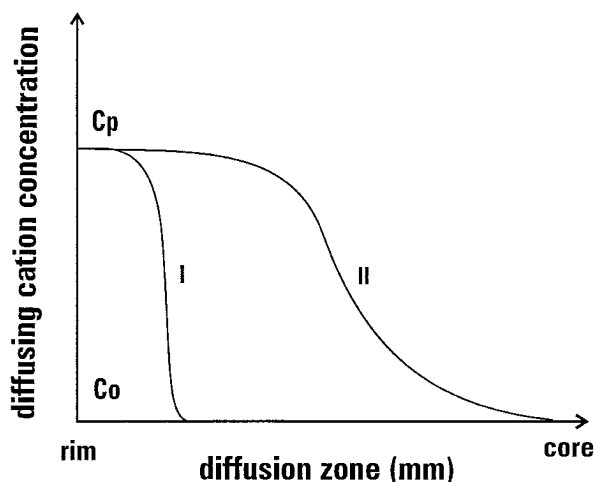


FIGURE 3. Schematic variation of the concentration profile of ingoing diffusing cations between crystal rim and crystal core for different diffusion times: (I) after short diffusion time and (II) after long diffusion time.

heating Na⁺-exchanged heulandite crystals in 2M potassium-, rubidium-, and cesium-chloride solutions. The solutions contained about a twenty-fold excess of the exchangeable cations. Under these conditions, the concentrations of cations were assumed to be constant on the surface of the exchanger, and film resistance can be ignored. During the exchange process, about 100 grains were taken from the solution at set intervals, washed with cold, distilled water, and dried in air at room temperature. The crystals were placed in an immersion liquid with a refractive index close to that of the crystals and all required measurements made within a few minutes.

During the exchange process, the chemical composition of the crystal rims changed because of cation diffusion. Consequently, the refractive indices and the optical orientation of the rims changed. Thus, in cross-polarized light, exchanged and non-exchanged areas of the crystal were distinguished by the variation of the extinction angle because the non- and cation-exchanged portions of the crystal went extinct at different settings of the microscope stage. In general, ten to fifteen grains with well-defined crystal edges and without cracks were selected for measurement of extinction angle differences. In this way, the dimension of the diffusion zone was measured directly with a calibrated, adjustable cross-hair by setting the non-exchanged crystal core at extinction (Fig. 2). Originally it was planned to determine the anisotropy of diffusion within the (010). We abandoned this idea because the diffusion zones appeared to be isotropic for all exchange experiments. Standard deviations for the length measurements were obtained from measurements in various plate directions and on various plates. It should be stressed that this method is only possible for crystals in the monoclinic or triclinic crystal system, because a variation in extinction angle with composition is possible. In addition, this technique is only applicable to crystals with a one- or

two-dimensional channel system where the channels are parallel to the crystal plates.

Exchanged Na, K, Rb, and Cs end-member heulandite samples used for measurement of optical properties and composition were prepared as described above (Yang and Armbruster 1996) but exchange times were lengthened and higher temperatures were used in the corresponding alkali-chloride solution. The composition of the natural heulandite and the exchanged samples were determined with a CAMECA SX50 electron microprobe operating at 20kV and 20 nA beam current and defocused beam diameter of about 20 μm to prevent sample destruction and loss of channel cations. Amelia albite was used as the standard for Na⁺, Al³⁺, and Si⁴⁺; orthoclase for K⁺; and anorthite for Ca²⁺. Synthetic RbVO₃ and CsVO₃ with a pyroxene structure (Hawthorne and Calvo 1977) were used as standards for Rb⁺ and Cs⁺.

It might be assumed that a cation diffusion zone in a single crystal could be measured directly by electron microprobe analyses as is done with other minerals. However, this technique has several shortcomings: (1) cation exchange occurs at relatively low temperature, thus zeolite samples must be transferred immediately to the electron microprobe, avoiding any time-consuming preparation techniques; (2) in the vacuum chamber and under electron bombardment, zeolites release H₂O, and cation diffusion occurs (Armbruster and Gunter 1991). For these reasons, we found electron microprobe analyses insufficient for a quantitative determination of diffusion zones.

Optical properties, 2V and indicatrix orientation, of exchanged 'end-member' heulandites were measured using spindle-stage extinction data and EXCALIBR (Bloss 1981; Gunter et al. 1988), and refractive indices were determined by the double-variation method (Bloss 1981; Su et al. 1987).

The exchange kinetics of the cation pairs 2 Na⁺ → Ca²⁺, K⁺ → Na⁺, Rb⁺ → Na⁺, and Cs⁺ → Na⁺, where the arrow head of a diffusion pair points to the cationic species replaced in the structural pores of heulandite, were studied at different temperatures. The exchange-diffusion coefficients (D) were calculated by the same method used by Tiselius (1934). First, given:

$$x = 2\beta\sqrt{Dt} \quad (1)$$

where, x is the diffusion distance of a cation at time t . Next, the parameter β is determined by:

$$\frac{C_p - C_x}{C_p - C_o} = \frac{2}{\sqrt{\pi}} \int_0^\beta e^{-\beta^2} d\beta \quad (2)$$

where, C_o is the concentration of the diffusion cation in a zeolite at the beginning of the exchange; C_p is the concentration of the cation in the completely exchanged zeolite; C_x is the concentration of the cation at the boundary of the exchange zone. The integral of Equation 2 has the characteristics of an error function (erf x) and was determined with a standard mathematical computer program or could be solved by use of Table 2.1 in Crank (1992).

The relation of cation concentration and diffusion zone

TABLE 1. Optical properties for natural and exchanged heulandite

	Natural	Na	K	Rb	Cs
α	1.4969	1.4865	1.4810	1.4854	1.5005
β	1.4992	1.4880	1.4835	1.4882	1.5007
γ	1.5046	1.4897	1.4878	1.4886	1.5104
mean n	1.5002	1.4881	1.4841	1.4874	1.5039
$2V_z$ (°)	63.5(7)	88.3(7)	69.0(2)	149.1(6)	18.2(2)
b	Z(AB)	Z(AB)	Y(ON)	Z(OB)	Z(AB)
$X \wedge c$ (°)	+11	-6	-1	+54	+100

is shown schematically in Figure 3. After a short reaction time a sharp diffusion zone forms that spreads out and becomes more diffuse after long diffusion times. Given a 2 μm error, which occurs as the diffusion zone spreads out, in the measurement of t in Equation 1, a resulting ca. 10% error would occur for D . The concentration of the ingoing cation at the boundary of the optically visible zone was assumed to be $C_x = (C_p - C_0)/2$. Given this assumption, β in Equation 2 equals 0.468984.

Although other diffusion models have been developed since the simple model of Tiselius (1934) that may better define diffusion in heulandite, these models are more complicated mathematically and may yield similar results. Many types of diffusion models exist in an attempt to account for the different variables that can occur in the system. For instance, some of the variables to consider are the different diffusion paths in a material (i.e., whether the diffusion is in a cylinder, a plane, or a sphere), infinite vs. semi-infinite diffusion, concentration-dependent diffusion, and the time dependence of diffusion (Crank 1992).

The validity of Tiselius's simple model (our Eq. 2) was tested by comparison with diffusion models given in Crank (1992) describing nonsteady radial diffusion in a cylinder. We tested two separate models, Equation 5.22 and 5.33 (Crank 1992), which describe cylindrical diffusion for longer and shorter periods of time, respectively. One problem with these equations is they require a size of the cylinder of diffusion and the diffusion depth to be given. For our case this would be the radius of the crystals, which varied slightly, thus average observed crystal size and diffusion depth were used. The $\text{K}^+ \rightarrow \text{Na}^+$ exchange data set was used to test these two models against that of Tiselius (1934). These models yield values of D approximately 70% higher and 35% lower, respectively, than Equation 2 (i.e., less than an order of magnitude difference). These differences are much lower than errors associated with other methods used to determine diffusion rates because of uncertainties in surface area measurements discussed earlier.

While selection of the an appropriate diffusion model is important to compare heulandite group zeolites with other materials, the main purpose of this project was to compare diffusion rates for different cations in this particular sample. Thus, we were more interested in diffusion rates in heulandite to gain a better understanding of the mechanism of cation diffusion and exchange rates

with this sample, than to determine absolute diffusion rates for comparison with other materials.

The activation energy (E_a) and thus the pre-exponential constant (D_0) can be calculated from the Arrhenius equation, $D = D_0 \exp(-E_a/RT)$ because a linear relationship exists between $\ln D$ and $1/T$. The entropy of activation ΔS^* was evaluated by:

$$D_0 = \frac{2.72kTd^2}{h} \exp\left(\frac{\Delta S^*}{R}\right) \quad (3)$$

where, k and h are the Boltzmann and Planck constants, respectively; R is the universal gas constant; d , the mean jump distance assigned a value of 5 Å (the approximate metal-metal distance in the channel); and T was assigned the standard value of 298 K (Barrer and Rees 1960).

RESULTS

The refractive indices, $2V$, and extinction angles of the natural sample and Na-, K-, Rb-, Cs-exchanged heulandite show distinct differences, particularly in the extinction angles (Table 1). Corresponding chemical analyses are given in Table 2. Thus, the exchange diffusion process of natural heulandite with Na^+ and Na-exchanged heulandite with K^+ , Rb^+ , and Cs^+ can be well-resolved with a polarizing microscope. A photomicrograph of Rb^+ diffusion into a Na-exchanged heulandite at 330 K after 24 h shows a light Rb^+ -exchanged rim and a dark core (Na-rich) where diffusion did not occur (Fig. 2). The diffusion front is about 96 μm .

Measurements of diffusion distances for exchange pairs as a function of time and temperature are summarized in Table 3. The exchange rates observed in heulandite single crystals are reasonably consistent with the \sqrt{t} law (Fig. 4) in agreement with previous diffusion studies on analcime (Barrer and Rees 1960), chabazite (Barrer et al. 1963), and mordenite (Rees and Rao 1966). Calculated diffusion parameters are listed in Table 4.

TABLE 2. Compositions of natural and exchanged samples

Sample	Composition
Natural heulandite	$\text{Na}_{0.96}\text{Ca}_{3.54}\text{K}_{0.09}(\text{Al}_{8.62}\text{Si}_{27.51}\text{O}_{72}) \cdot n\text{H}_2\text{O}$
Na-exchanged heulandite	$\text{Na}_{5.83}\text{Ca}_{1.18}\text{K}_{0.01}(\text{Al}_{8.65}\text{Si}_{27.47}\text{O}_{72}) \cdot n\text{H}_2\text{O}$
K-exchanged heulandite	$\text{K}_{8.64}\text{Na}_{0.03}\text{Ca}_{0.01}(\text{Al}_{8.65}\text{Si}_{27.34}\text{O}_{72}) \cdot n\text{H}_2\text{O}$
Rb-exchanged heulandite	$\text{Rb}_{8.54}\text{Na}_{0.01}\text{Ca}_{0.18}(\text{Al}_{8.80}\text{Si}_{27.17}\text{O}_{72}) \cdot n\text{H}_2\text{O}$
Cs-exchanged heulandite	$\text{Cs}_{8.36}\text{Na}_{0.03}\text{Ca}_{0.29}(\text{Al}_{8.80}\text{Si}_{27.16}\text{O}_{72}) \cdot n\text{H}_2\text{O}$

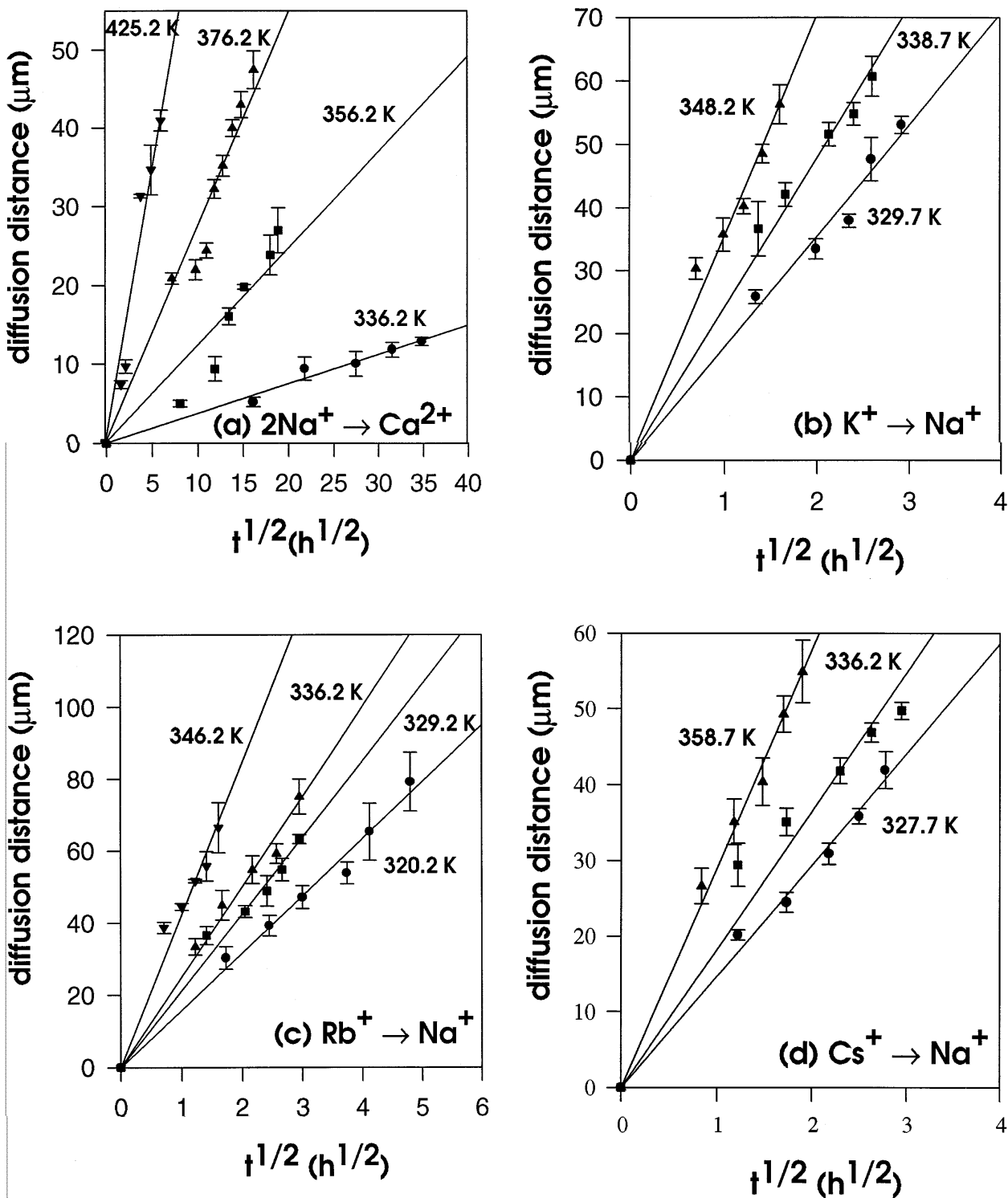


FIGURE 4. Average diffusion distance measurements with the polarizing microscope vs. the square root of diffusion time at various temperatures. Solid lines result from a linear regression forced through the origin: (a) $2\text{Na}^+ \rightarrow \text{Ca}^{2+}$, (b) $\text{K}^+ \rightarrow \text{Na}^+$, (c) $\text{Rb}^+ \rightarrow \text{Na}^+$, (d) $\text{Cs}^+ \rightarrow \text{Na}^+$. Error bars are the standard deviation for the ten to fifteen heulandite crystals measured for each condition.

TABLE 3. The location of the diffusion front for the different experimental conditions

Reaction	T(K)	t(h)	Distance (μm)
$2\text{Na}^+ \rightarrow \text{Ca}^{2+}$	336.2	264.0	5.2(6)
		480.0	9.4(15)
		760.5	10.1(15)
		1001.0	11.8(9)
		1219.5	12.9(5)
		67.0	5.0(4)
	356.2	144.5	9.4(16)
		184.0	16.1(11)
		232.0	19.8(3)
		328.0	23.8(25)
		360.0	26.9(28)
		53.0	20.8(7)
	376.2	97.5	22.0(12)
		122.5	24.4(10)
		142.5	32.2(12)
		166.5	35.2(13)
		194.5	40.0(11)
		221.0	43.0(16)
	425.2	264.5	47.5(24)
		3.0	7.4(5)
		5.0	9.7(8)
		15.0	31.3(2)
		25.0	34.7(31)
		37.0	41.0(14)
$\text{K}^+ \rightarrow \text{Na}^+$	329.7	1.8	25.8(11)
		4.0	33.4(16)
		5.6	37.9(11)
		6.8	47.7(34)
	338.7	8.6	53.1(14)
		1.9	36.7(43)
		2.8	42.1(18)
		4.6	51.6(19)
	348.2	5.8	54.8(18)
		6.8	60.7(31)
		0.5	30.3(17)
		1.0	35.8(26)
$\text{Rb}^+ \rightarrow \text{Na}^+$	320.2	1.5	40.2(12)
		2.0	48.6(15)
		2.6	56.3(31)
		3.0	30.3(31)
	329.2	6.0	39.3(29)
		9.0	47.2(32)
		14.0	53.8(30)
		17.0	65.3(80)
	336.2	23.0	79.2(82)
		2.0	36.6(25)
		4.2	43.2(17)
		5.8	48.9(42)
348.2	7.1	54.8(31)	
	8.7	63.2(12)	
	1.5	34.0(23)	
	2.8	45.0(41)	
358.7	4.7	54.8(38)	
	6.6	59.3(27)	
	8.7	75.1(49)	
	0.5	38.7(15)	
$\text{Cs}^+ \rightarrow \text{Na}^+$	327.6	1.0	44.5(10)
		1.5	51.8(5)
		2.0	55.8(40)
		2.6	66.5(70)
	336.2	1.5	20.2(7)
		3.0	24.5(13)
		4.8	30.9(14)
		6.3	35.8(11)
	358.7	7.8	41.9(24)
		1.5	29.4(28)
		3.0	35.1(18)
		5.3	41.8(17)
366.2	6.9	46.9(13)	
	8.7	49.7(12)	
	0.7	26.6(23)	
	1.4	35.1(30)	
374.2	2.2	40.4(31)	
	2.9	49.3(24)	
	3.6	54.9(42)	

TABLE 4. Calculated rates for exchange diffusion

Reaction	T (K)	D (cm^2/s)	E_a (kJ/mol)	D_0 (cm^2/s)	ΔS (J/mol·K)
$2\text{Na}^+ \rightarrow \text{Ca}^{2+}$	336.2	2.0×10^{-13}	78.5	0.507	20.66
	356.2	2.0×10^{-12}			
	376.2	1.1×10^{-11}			
	425.2	8.0×10^{-11}			
$\text{K}^+ \rightarrow \text{Na}^+$	329.7	9.6×10^{-10}	69.6	98.57	64.47
	338.7	1.7×10^{-9}			
	348.2	3.7×10^{-9}			
	320.2	7.8×10^{-10}			
$\text{Rb}^+ \rightarrow \text{Na}^+$	329.2	1.4×10^{-9}	61.7	8.66	44.25
	336.2	1.9×10^{-9}			
	348.2	5.2×10^{-9}			
	327.6	6.6×10^{-10}			
$\text{Cs}^+ \rightarrow \text{Na}^+$	336.2	9.6×10^{-10}	42.1	0.0034	-20.98
	358.7	2.5×10^{-9}			

DISCUSSION

Comparing mean refractive indices (\bar{n}) of exchanged heulandites (Table 1), one may be surprised at the lack of a linear trend between the atomic number of channel cations and \bar{n} . The mean refractive index of K- and Rb-exchanged heulandite is smaller than that for Na-exchanged heulandite. The key to understanding this supposed discrepancy is the increasing ionic radius from Na^+ to Cs^+ . The larger the channel cation is, the less H_2O is incorporated into the structural pores, resulting in lower \bar{n} values. An estimate of the H_2O content can be derived from the 100 K crystal structure data of the corresponding samples (Yang and Armbruster 1996) where 21.5, 19.0, 17.5, and 12.5 H_2O p.f.u. were refined for Na-, K-, Rb-, and Cs-exchanged heulandite, respectively. A natural Ca-rich heulandite from Poona (India) with a similar chemical composition as the Nasik sample used in this study has 21.4 H_2O p.f.u. (Gunter et al. 1994). This relation between cation size and degree of hydration has a direct bearing on the exchange experiment (e.g., the exchange of Na^+ by Cs^+ is not a simple $\text{Cs}^+ \rightarrow \text{Na}^+$ reaction but may be written more accurately as $\text{Cs}^+ \rightarrow \text{Na}^+ + \text{H}_2\text{O}$); thus the diffusion of H_2O also plays a role in cation diffusion.

The diffusion of H_2O in heulandite is strongly anisotropic. The (001) face described by Tiselius (1934) corresponds to (100) in the cell setting used here with $a = 17.7$, $b = 17.9$, $c = 7.4 \text{ \AA}$, $\beta = 116^\circ$. This crystal face gives no access to the A or B channels which are parallel to this face, while the other faces studied by Tiselius (1934) do give access to A and B channels. Below 300 K the diffusion coefficients inclined to the (100) face are approximately one order of magnitude higher than perpendicular to (100). At higher temperature (but $< 350 \text{ K}$) the diffusion coefficients become more similar. The activation energies for H_2O diffusion into heulandite are 21.3 kJ/mol [inclined to (100)] and 38.3 kJ/mol [perpendicular to (100)]. On the basis of the crystal structure (not known at the time of the Tiselius study), the anisotropy of H_2O diffusion indicates that H_2O prefers the A channels for diffusion. The A channels are not as strongly blocked by cations as the B and C channels (e.g., Gunter et al. 1994;

Yang and Armbruster 1996). In contrast to the strongly anisotropic H₂O diffusion, we find no significant anisotropy for the cation exchange diffusion.

Tarasevich et al. (1988) measured thermodynamic parameters for Li⁺, NH₄⁺, K⁺, Rb⁺, and Cs⁺ diffusing into previously Na-exchanged, microcrystalline clinoptilolite. Clinoptilolites, although structurally identical to heulandite, have less Al substituted in the tetrahedral framework. Thus fewer exchangeable cations obstruct the channels, increasing the diffusion rates. These authors argue that the exchange enthalpies control the observed equilibrium constant. ΔH_{exch} decreases from K⁺ → Na⁺_{clino} (−17.6 kJ/mol), Rb⁺ → Na⁺_{clino} (−21.8 kJ/mol), to Cs⁺ → Na⁺_{clino} (−23.7 kJ/mol). As a reason for the low energy of a Cs⁺ → Na⁺ exchange, they suggest that the large cations (Cs⁺, Rb⁺) interact with more O atoms on the channel surface.

A simple model for cation selectivity was introduced by Eisenman (1962) for glass electrodes and extended to zeolites by Sherry (1969): the preference of the exchanger for one cation over another depends on whether the difference in their hydration free energies or their Coulombic energies of interaction with the fixed anionic exchange sites predominates. On the basis of this theory, a diagram of free energy of exchange of alkali metal ions for Na⁺ as a function of anionic field strength can be calculated. A certain field strength corresponds to a certain selectivity series. Heulandite and clinoptilolite are low field strength zeolites (the Si/Al ratio is relatively high) for which the theory predicts a selectivity series of type I (Cs⁺ > Rb⁺ > K⁺ > Na⁺ > Li⁺) which has been confirmed experimentally (Ames 1960) for clinoptilolite. The selectivity of a zeolite structure under equilibrium is not simply related to the diffusion rate (e.g., in mordenite the selectivity series is Cs⁺ > Rb⁺ > K⁺ > Na⁺) but the diffusion constants of alkali ions diffusing into Na mordenite show the sequence $D_{\text{Rb}} > D_{\text{K}} > D_{\text{Cs}}$ (Rao and Rees 1966). Diffusion rates are mainly governed by dispersion-repulsion, Coulombic forces, and the pathways available to specific ions.

On the basis of our own findings and literature data, a preferred exchange mechanism, though highly simplified, can be suggested for K⁺ and Rb⁺ exchange with Na-rich heulandite. The ingoing cations will preferentially approach the channel system through the eight-membered rings (both B and C). This is supported by: (1) crystal structure analyses (Yang and Armbruster 1996) showing that these ring sites have the highest population of channel cations, (2) the isotropy of exchange diffusion in (010) heulandite plates, and (3) the experiments by Tarasevich et al. (1988). All channels limited by eight-membered tetrahedral rings (B, C) have eight-membered ring connections allowing access to the neighboring ten-membered tetrahedral ring A channel. If the ingoing cations seem to avoid the A channels, then this channel may be the preferred path of the outgoing ions to leave the structure. Tiselius (1934) showed with his single-crystal diffusion experiments that H₂O preferentially diffuses parallel to the A channel. This is in agreement with

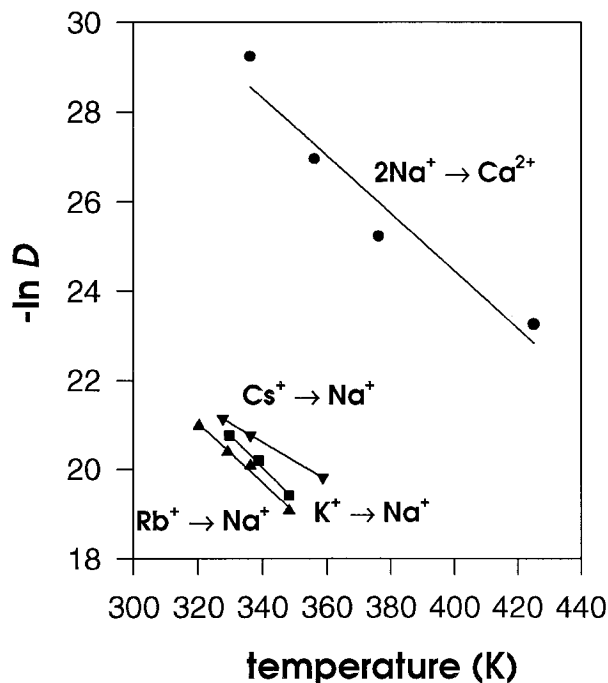


FIGURE 5. The relationship of diffusion coefficients and temperature for the exchange experiments.

Tarasevich et al. (1988) who propose that Na⁺ will diffuse as a water complex (Na [H₂O]_n)⁺ to avoid Coulomb interactions with the channel surface. This is also supported by the higher degree of hydration of the Na-exchanged sample compared with the K-, Rb-, and Cs-exchanged samples. Tarasevich et al. (1988) assumed that Cs⁺ in clinoptilolite also diffuses through the ten-membered rings, while K⁺ and Rb⁺ enter the structural pores preferentially through eight-membered rings.

The relation of diffusion coefficients to temperature for exchange experiments show the diffusion rate for Na⁺ into natural, Ca-rich heulandite is sluggish in comparison with the rates of K⁺, Rb⁺, and Cs⁺ diffusion into Na-rich heulandite (Fig. 5). At 336 K, the diffusion coefficient for Na⁺ into natural heulandite is almost 10⁴ times smaller than for the exchanges K⁺ → Na⁺ and Rb⁺ → Na⁺, and almost 5 × 10³ times smaller than the one of Cs⁺ → Na⁺ (Table 4). Barrer and Rees (1960) and Barrer et al. (1963) pointed out that diffusion exchange depends on two factors: (1) the size of the cation relative to the free diameter of the channels of zeolite and (2) the charge of the cation. For the exchange process of K⁺, Rb⁺, and Cs⁺ with Na-exchanged heulandite, the exchanged Na⁺ can more easily diffuse away because the interactive force (Coulombic attraction) between monovalent Na⁺ and the framework is relatively weak. However, there is a relatively stronger Coulombic attraction between the divalent Ca²⁺ and the framework of the zeolite, and thus the diffusion coefficient of Na⁺ → Ca²⁺ is much smaller than that of alkali group cations exchanging with Na-filled heulandite.

Within the experimental temperature range (320–425 K), the diffusion coefficients for alkali cations into Na-exchanged heulandite show the sequence $D_{\text{Rb}} > D_{\text{K}} > D_{\text{Cs}}$ (Table 4). This is the same sequence of diffusion rates as for Rb^+ , K^+ , and Cs^+ in Na-filled mordenite (Rao and Rees 1966), though the diffusion in heulandite is considerably faster because of the higher number of intersecting channels. However Barrer and Rees (1960) found $D_{\text{K}} > D_{\text{Rb}} > D_{\text{Cs}}$ for analcime, and Barrer et al. (1963) found $D_{\text{Cs}} > D_{\text{K}} > D_{\text{Rb}}$ for chabazite. These differences in the D between the different zeolites can be attributed to channel dimensions. The channels in chabazite have a free diameter of approximately of 3.8 Å (Meier and Olson 1992), which permits Cs^+ diffusion.

Although the main purpose of our experiments was to determine the relative rates of cation exchange within heulandite, it is interesting to compare our heulandite diffusion results with those performed on analcime (Barrer and Rees 1960), chabazite (Barrer et al. 1963), and mordenite (Rao and Rees 1966). The overall diffusion values for all cations are $D_{\text{Heu}} > D_{\text{Cha}} > D_{\text{Mor}} > D_{\text{Ana}}$. In general these results are not surprising. Heulandite has the largest, most open channels, and analcime has the smallest. The channel size in mordenite is larger than in both heulandite and chabazite, but the channels are offset, and thus their free aperture is reduced by one half (Rao and Rees 1966). However, it should be noted that even another heulandite, with say different Si-Al ordering or a different Si/Al ratio, would have different values of D . For instance, the higher the Si/Al ratio, the lower the Coulombic force, and larger values of D would be expected. This is one reason why clinoptilolite, which as a higher Si/Al ratio than heulandite, has better cation exchange properties.

The free diameters of channel A, B, and C for heulandite are about 7.6×3.0 Å, 4.6×3.3 Å, and 2.9×4.7 Å, respectively (Meier and Olson 1992), whereas the diameters of alkali cations are 1.90, 2.66, 2.96, and 3.38 Å, increasing from Na^+ to K^+ to Rb^+ to Cs^+ . It seems that the large radius of Cs^+ and its associated hydration sphere prevent rapid diffusion through the heulandite channels. A structural refinement revealed that there are four main cation sites in Cs-exchanged heulandite (Yang and Armbruster 1996). In order to occupy these sites, Cs^+ can diffuse through any of the three channel types (Fig. 1). If Cs^+ cannot pass through the small aperture of the eight-member rings forming the C channels, which is the smallest open diameter in the structure, the diffusion of Cs^+ in heulandite should be strongly anisotropic because the larger, and thus more favorable, A and B channels extend parallel to the c axis. However, no obvious indication of anisotropic diffusion was observed. In our experimental conditions this indicates that the diameters of heulandite channels, and also the diameters of exchanging cations, can distort to allow Cs^+ diffusion. The C channel is the narrowest parallel to b . Cell dimensions of exchanged heulandites measured at 100 K (Yang and Armbruster 1996) reveal that the b axis increases from 17.93 Å (Na-exchanged heulandite) to 18.10 Å (Cs-exchanged

heulandite), supporting the assumed flexibility of the tetrahedral framework. Thus the C channel may retard the diffusion of Cs^+ in Na-exchanged heulandite but does not prevent Cs^+ from diffusing into the crystals.

The activation energies for the exchange diffusion are 69.6, 61.7, and 42.1 kJ/mol for $\text{K}^+ \rightarrow \text{Na}^+$, $\text{Rb}^+ \rightarrow \text{Na}^+$, and $\text{Cs}^+ \rightarrow \text{Na}^+$, respectively. Following the arguments by Rees and Rao (1966) for alkali self-diffusion in mordenite, comparable figures for K^+ and Rb^+ suggest that the interaction is mainly Coulombic because these cations are smaller than the channel diameters in heulandite. Rees and Rao (1966) suggest Coulombic forces predominate when the cations are smaller than the channel free-diameter, while dispersive-repulsion forces predominate when the cations are larger than the channel-free diameter. The low value of 42.1 kJ/mol implies a different mechanism for Cs^+ diffusion in Na-exchanged heulandite.

The activation entropy (Table 4) describes the entropy difference between a ground state (roughly known by crystal structure analyses) and the transition complex (unknown). In our case the transition complex may have different properties because it involves the incoming and outgoing cations including their coordination sphere, H_2O molecules in the structural channels and the rings, and the channel surface built by $(\text{Si},\text{Al})\text{O}_4$ tetrahedra. We may assume that the transition complex has either more or less degrees of freedom than the ground state. If the transition state has more degrees of freedom than the ground state, the activation entropy becomes positive and vice versa.

The activation entropies calculated for $2\text{Na}^+ \rightarrow \text{Ca}^{2+}$, $\text{K}^+ \rightarrow \text{Na}^+$ and $\text{Rb}^+ \rightarrow \text{Na}^+$ are positive. Positive entropies have been interpreted as “window effects” by Rees and Rao (1966). The vibrational freedom of the O atoms making up tetrahedral rings is reduced because the exchanged cations sit in the rings confining the channels. If the exchanged cation moves from the center of the tetrahedral ring, the entropy is increased because the electrons of the O atoms can move into the open ring (Rees and Rao 1966). Structural refinements prove that Ca^{2+} in natural heulandite and Na^+ in Na-exchanged heulandite prefer ring sites (Gunter et al. 1994). However, the entropy of activation calculated for $\text{Cs}^+ \rightarrow \text{Na}^+$ is negative. This has been ascribed to a cooperative movement of O atoms of the framework and H_2O molecules to facilitate the diffusion-jump process (Barrer et al. 1963).

REFERENCES CITED

- Ames, L.L., Jr. (1960) The cation sieve properties of clinoptilolite. *American Mineralogist*, 45, 689–700.
- (1962) Effect of base cation on the cesium kinetics of clinoptilolite. *American Mineralogist*, 47, 1310–1316.
- Armbruster, T. and Gunter, M.E. (1991) Stepwise dehydration of a heulandite-clinoptilonite from Succor Creek, Oregon, U.S.A.: A single-crystal X-ray study at 100 K. *American Mineralogist*, 76, 1872–1883.
- Barrer, R.M. and Hinds, L. (1953) Ion-exchange in crystals of analcime and leucite. *Journal of the Chemical Society*, 1879–1888.
- Barrer, R.M. and Munday, B.M. (1971a) Cation exchange reactions of zeolite Na-P. *Journal of the Chemical Society (A)*, 2909–2914.

- (1971b) Cation exchange in the synthetic zeolite K-F. *Journal of the Chemical Society (A)*, 2914–2921.
- Barrer, R.M. and Rees, L.V.C. (1960) Self-Diffusion of alkali metal ions in analcite. *Transactions of the Faraday Society*, 56, 709–721.
- Barrer, R.M., Bartholomew, R.F., and Rees, L.V.C. (1963) Ion exchange in porous crystals part I. self- and exchange-diffusion of ions in chabazites. *Journal of Physics and Chemistry of Solids*, 24, 51–62.
- Barrer, R.M., Papadopoulos, R., and Rees, L.V.C. (1967) Exchange of sodium in clinoptilolite by organic cations. *Journal of Inorganic and Nuclear Chemistry*, 29, 2047–2063.
- Bloss, F.D. (1981) *The spindle stage: Principles and practice*, 340 p. Cambridge University Press, Cambridge, U.K.
- Breck, D.W. (1974) *Zeolite molecular sieves: structure, chemistry, and use*. 188 p. Wiley, New York.
- Crank, J. (1992) *The Mathematics of Diffusion*. 414 p. Oxford Science Publications, Oxford.
- Eisenman, G. (1962) Cation selective glass electrodes and their mode of operation. *Biophysical Journal Supplements*, 2, 259–323.
- Gunter, M.E., Bloss, F.D., and Su, S.C. (1988) EXCALIBUR revisited. *American Mineralogist*, 73, 1481–1482.
- Gunter, M.E., Armbruster, T., Kohler, T., and Knowles, C.R. (1994) Crystal structure and optical properties of Na- and Pb-exchanged heulandite-group zeolites. *American Mineralogist*, 79, 675–682.
- Hawthorne, F.C. and Calvo, C. (1977) The crystal chemistry of the M^+VO_3 ($M^+ = Li, Na, K, NH_4, Tl, Rb$ and Cs) pyroxenes. *Journal of Solid State Chemistry*, 22, 157–170.
- Koyama, K. and Takéuchi, Y. (1977) Clinoptilolite: the distribution of potassium atoms and its role in thermal stability. *Zeitschrift für Kristallographie*, 145, 216–239.
- Meier, W.M. and Olson, D.H. (1992) Atlas of zeolite structure types. *Zeolites*, 12, 449–654.
- Merkle, A.B. and Slaughter, M. (1968) Determination and refinement of the structure of heulandite. *American Mineralogist*, 53, 1120–1138.
- Mumpton, F.A. (1988) Development of uses for natural zeolites: A critical commentary. In Kallo, D., and Sherry, H.S., Eds., *Occurrence, properties, and utilization of natural zeolites*, p. 333–365. Akadémiai Kiado, Budapest, Hungary.
- Rao, A. and Rees, L.V.C. (1966) Kinetics of ion exchange in mordenite. *Transactions of the Faraday Society*, 62, 2505–2512.
- Rees, L.V.C. and Rao, A. (1966) Self-diffusion of various cations in natural mordenite. *Transactions of the Faraday Society*, 62, 2103–2110.
- Sherry, H.S. (1966) The ion-exchange properties of zeolites. I. Univalent ion exchange in synthetic faujasite. *Journal of Physical Chemistry*, 70, 1158–1168.
- H.S. (1969) The ion-exchange properties of zeolites. In Manisky, J.A., and Dekker, M., Eds., *Ion exchange*, p. 89–133. Marcel Dekker, New York.
- Smyth, J.R., Spaid, A.T., and Bish, D.L. (1990) Crystal structures of a natural and a Cs-exchanged clinoptilolite. *American Mineralogist*, 75, 522–528.
- Su, S.C., Bloss, F.D., and Gunter, M.E. (1987) Procedures and computer programs to refine the double variation method. *American Mineralogist*, 72, 1011–1013.
- Sukheswala, R.N., Avasia, R.K., and Gangopadhyay, M. (1974) Zeolites and associated secondary minerals in the Deccan Traps of Western India. *Mineralogical Magazine*, 39, 658–671.
- Tarasevich, Yu.I., Polyakov, V.E., and Badekha, L.I. (1988) Structure and localization of hydrated alkali, alkali earth and transition metal cations in clinoptilolite determined from ion-exchange, calorimetric and spectral measurements. In Kallo, D., and Sherry, H.S., Eds., *Occurrence, properties and utilization of natural zeolites*, p. 421–430. Akadémiai Kiado, Budapest, Hungary.
- Tiselius, A. (1934) Die Diffusion von Wasser in einem Zeolithkristall. *Zeitschrift für Physikalische Chemie*, 169 A, 425–458.
- Yang, P. and Armbruster, T. (1996) Na, K, Rb, and Cs exchange in heulandite single-crystals: X-ray structure refinements at 100 K. *Journal of Solid State Chemistry*, 123, 140–149.

MANUSCRIPT RECEIVED NOVEMBER 21, 1995

MANUSCRIPT ACCEPTED FEBRUARY 4, 1997